Chelate titrations of Ca^{2+} and Mg^{2+} using microfluidic paper-based analytical devices

Shingo Karita and Takashi Kaneta*

Department of Chemistry, Graduate School of Natural Science and Technology, Okayama University, Okayama 700-8530, Japan

E-mail: kaneta@okayama-u.ac.jp. Tel: +81-86-251-7847. Fax: +81-86-251-7847.

ABSTRACT

We developed microfluidic paper-based analytical devices (μPADs) for the chelate titrations of Ca^{2+} and Mg^{2+} in natural water. The μPAD consisted of ten reaction zones and ten detection zones connected through narrow channels to a sample zone located at the center. Buffer solutions with a pH of 10 or 13 were applied to all surfaces of the channels and zones. Different amounts of ethylenediaminetetraacetic acid (EDTA) were added to the reaction zones and a consistent amount of a metal indicator (Eriochrome Black T or Calcon) was added to the detection zones. The total concentrations of Ca^{2+} and Mg^{2+} (total hardness) in the water were measured using a μPAD containing a buffer solution with a pH of 10, whereas only Ca^{2+} was titrated using a μPAD prepared with a potassium hydroxide solution with a pH of 13. The μPADs permitted the determination of Ca^{2+} and Mg^{2+} in mineral water, river water, and seawater samples within only a few minutes using only the naked eye — no need of instruments.

1. Introduction

Since the first demonstration by Whitesides' group in 2007 [1], microfluidic paper-based analytical devices (μPADs) have gained a significant amount of attention as an analytical platform. Several publications have recognized μPADs that are fabricated from paper substrates as suitable for point–of–care testing and on–site analysis [2-4], because they are easy to fabricate, light, inexpensive, disposable, transportable, and instrument-free.

As seen in a recent review article on μPADs [5], several detection methods including colorimetry [6-8], electrochemistry [9-11], fluorometry [12], chemiluminescence [13,14], and electrochemiluminescence [15], have been reported in the past decade. Among them, colorimetry is the most popular detection scheme whereby a scanner or digital camera captures the color image of a μPAD, followed by a measurement of the color intensity using image-processing software [7,16-19]. For the purpose of point–of–care testing, smart phones are coupled with μPADs since smart phones are equipped with both a camera and image-processing software in a small package [20].

Conversely, the naked eye is a potentially excellent detector, as we demonstrated in a previous study on μPADs used for acid-base titrations [21]. Using the μPADs, the endpoint of the neutralization reaction can be visualized by a color change in the detection zone adjacent to the reaction zone containing an equivalent amount of titrant. The first attempt at using the naked eye was in distance-based detection, which was developed by Henry's group [22]. The length-based detection scheme permitted the determinations of glucose, glutathione, nickel ion [22], and lactoferrin [23]. With these methods, the concentration of an analyte was determined by the length of the

colored channel that became elongated with increases in its concentration.

In our previous research, we demonstrated acid-base titrations on μPADs consisting of ten reaction zones and ten detection zones [21]. Strong and weak acids and bases could be titrated by selecting an appropriate indicator. The principle would obviously be applicable to other classic titration methods that include chelate titrations, redox titrations, and precipitation titrations. Although the detection scheme is slightly different, iodometry was demonstrated as an example of redox titrations [24]. In addition, acid-base titrations were achieved using another type of paper-based device, which was constructed by stacking two conventional PADs on top of one another and bonding them together [25]. As seen in these articles, μPAD-based titrations are expected to be an alternative to classic titration techniques since they simplify the operations, reduce consumption of the reagents, facilitate on-site-analysis, and are free from treatment of waste solutions after titrations due to possible incineration disposal.

In the present study, we developed μPADs for chelate titrations of Ca^{2+} and Mg^{2+} using ethylenediaminetetraacetic acid (EDTA) according to the same principle as that previously reported for acid-base titrations. Several factors including selection of the buffer components and the indicator, amounts of chemicals added to the μPAD, and the channel length were optimized to obtain accurate and precise analytical results. The developed μPADs were successfully applied to the rapid determinations of Ca^{2+} and Mg^{2+} in mineral water, river water, and seawater samples.

2. Experimental

2.1. Chemicals

Deionized water was prepared by means of an Elix water purification system (Millipore

Co. Ltd., Molsheim, France). N-Cyclohexyl-3-aminopropanesulfonic acid (CAPS) was obtained from Dojindo Molecular Technologies, Inc. (Kumamoto, Japan). Magnesium sulfate, calcium chloride dihydrate, sodium hydroxide, iron(III) standard solution (1000 ppm), 1-(2-hydroxy-1-naphthylazo)-2-naphthol-4-sulfonic acid sodium salt (Calcon), and 2-hydroxy-1-(2-hydroxy-4-sulfo-1-naphthylazo)-3-naphthoic acid (NN) were purchased from Wako Pure Chemical Industries (Osaka, Japan). Ammonium chloride, ammonium hydroxide solution, potassium cyanide, and Eriochrome Black T (EBT) were obtained from Kanto Chemical (Tokyo, Japan). Ethylenediaminetetraacetic acid, disodium salt (EDTA・2Na) and methanol were purchased from Sigma–Aldrich (St. Louis, MO, USA). All indicators were dissolved in methanol at a concentration of 0.1 (w/v)%. A buffer solution with a pH of 10 was prepared by dissolving appropriate amounts of CAPS in water and adjusting the pH with a sodium hydroxide solution.

2.2. Fabrication and preparation of the μPADs

The structure of the μPAD employed in this study was similar to that reported previously [21] except for the channel length between the reaction and detection zones (Supplementary Material, Fig. S1). Microsoft Office Power Point 2010 was used to design the μPADs with a sample zone located at the center and ten reaction and detection zones each arranged radially in a 30 × 30 mm square. According to a method developed by Carrilho and co-workers, the designed μPADs were printed on a sheet of filter paper (200 × 200 mm, Chromatography Paper 1CHR, Whatman, GE Healthcare Lifesciences, United Kingdom) using a wax printer (ColorQube 8570DN, Xerox, CT, USA) [26] followed by heating at 120 °C for 3 min in a drying machine (ONW-300S, AS ONE Corporation, Osaka, Japan). The back of the printing surface was covered with

transparent packing tape to prevent solutions from leaking from beneath the μPAD.

Each μPAD was cut into a piece that measured 30 × 30 mm, and then 30 μL of the buffer solution (pH 10 or 13) was added to the sample zone so as to completely fill the surfaces of the channels and zones of the μPAD (30 μL is the volume needed to fill all hydrophilic channels and zones [21]). The μPAD was completely dried, and then a 1 μL solution of ten different EDTA concentrations was added to each of the reaction zones since the volume needed to fill a reaction zone was determined to be 1 μL as reported in the previous paper [21], and 0.5 μL of a 0.1(w/v)% indicator solution was added to each of the detection zones. To accomplish titration, the μPAD was placed on an acrylic plate holder that was composed of two 30 × 30 mm plates with four fins at the corners of the holder in order to avoid bending of the μPAD (Supplementary Material, Fig. S1). Finally, a micropipette was used to introduce 30 μL of the sample solution from the center of the μPAD.

2.3. Principle of chelate titrations using the μPADs

The principle of chelate titrations is similar to that of classic chelate titrations for Ca^{2+} and Mg^{2+} with EDTA, wherein the total concentration is determined at pH 10, whereas only Ca^{2+} is titrated at pH 13 since Mg^{2+} is masked with hydroxide ion so as not to react with EDTA [27]. However, in contrast to the classic titrations, the concentrations of Ca^{2+} and Mg^{2+} are directly determined by finding the endpoint from the color change without either calibration or calculation when using the μPAD method. When a sample solution is introduced into the center of the μPAD, the sample solution penetrates into ten reaction zones. Then, 1 μL of the sample solution can react with EDTA at each reaction zone since the volume occupying the reaction zone is 1 μL, which is the same

as the volume of EDTA solutions added to the reaction zones. So, when the amount of metal ions exceeds that of the EDTA in the reaction zones, uncomplexed metal ions penetrate the detection zones, resulting in a color reaction of blue (free form) to purple (complex with metal ion) from the indicator. The concentration of the metal ion is equivalent to the lowest EDTA concentration of the reaction zone among those adjacent to the detection zones with blue color, which indicates no influx of the uncomplexed metal ions. Therefore, in the proposed method, we need to know only the exact concentrations of EDTA added to the reaction zones without further calibration.

2.4. Practical samples

Bottles of commercially available mineral water were purchased at a local supermarket. Natural water samples were taken from the Asahigawa River, from Kojima Bay, and from the Shimotsui Fishery Harbor in Okayama Prefecture, Japan. The sample solutions were kept in plastic bottles and were determined in our laboratory. The sample solutions were titrated with EDTA via both the classic titration method and the μPADs in order to evaluate the accuracy and precision of the μPADs.

3. Results and Discussion

3.1. Selection of the reagents

In a classic chelate titration of Ca^{2+} and Mg^{2+} with EDTA, the total concentration is determined using an ammonia buffer at pH 10, whereas only Ca^{2+} is titrated at a pH of 13 that is adjusted with KOH to buffer the pH and mask the Mg^{2+}. However, volatile ammonia is unsuitable for use in μPADs since reagent solutions added to the μPAD must be dried before use, which results in a change in the pH value due to the

volatilization of ammonia.

A buffer that would be suitable for use in μPADs should have a pK_a value that is near the selected pH and should be a stable solid at room temperature. We selected the CAPS buffer to accomplish a pH of 10 since the pK_a value of CAPS is 10.6, whereas KOH was employed for the buffer at pH 13. These buffer components are solid so that the pH could be adjusted to 10 and 13, although exposure to CO_2 under air should be avoided in order to maintain an alkaline pH. Thus, the μPADs should be stored with either vacuum-sealed or nitrogen-substitution packaging.

In a classic chelate titration for Ca^{2+} and Mg^{2+}, EBT is used as the indicator at pH 10, while NN permits the determination of only Ca^{2+} at pH 13 [28]. Both EBT and NN change from blue to purple via the formation of a complex with Ca^{2+} and Mg^{2+} in different pH regions because of their different p*K*a values. Therefore, EBT and NN are employed as the indicators at pH 10 and 13, respectively, in classic titrations.

In the preparation of the μPAD for the chelate titration at pH 10, we added 0.1 M CAPS buffer to completely fill the channels and zones. When 0.1% EBT was dropped into the detection zones containing 0.1 M CAPS buffer, the EBT showed a clear blue color. Thus, EBT worked well as the indicator in the presence of the CAPS buffer, pH 10, when using the μPAD. However, when 0.1% NN was dropped into the detection zone of a μPAD with the pH adjusted to 13 using 0.1 M KOH, no color was observed, despite the presence or absence of metal ions (Fig. 1) — i.e., the NN was unsuitable due to its low color intensity when using the μPAD. Therefore, instead of NN, we examined EBT and Calcon at pH 13 since their structures are similar to NN, with the exception of a substituted functional group (Supplementary Material, Fig. S2).

Surprisingly, the blue color of EBT without Ca^{2+} persisted on the filter paper even in

the presence of 0.1 M KOH (Fig. 1), despite a purple color in solution. The purple color of EBT at pH 13 was quite reasonable since the pK_{a2} value was 11.6 [27], because more than 98% of EBT is a trivalent anionic species (purple color). When adding Ca^{2+} and Mg^{2+} into the solution, the purple color persisted, which meant that EBT was unsuitable as an indicator in the solution with a pH of 13.

The fact that EBT exhibited a blue color in the presence of 0.1 M KOH implied some interaction between EBT and the paper substrate. One possible explanation could be the interaction of the dissociated hydroxyl group of EBT with the hydroxyl groups of the paper substrate, cellulose. The color of EBT should change from purple to blue when one of the dissociated hydroxyl groups is protonated. Therefore, on the paper substrate, the dissociated hydroxyl group may have interacted with the hydroxyl groups of the cellulose. As a result, EBT may show a blue color on filter paper containing 0.1 M KOH, although its color was purple in a solution with a pH of 13.

Unfortunately, EBT was unsuitable for use at a pH of 13 since it changed color in the presence of Mg^{2+} (Fig. 1), which could have been due to the complex formation of Mg^{2+} with EBT. Conversely, a change in the color of Calcon was observed only when adding Ca^{2+}, whereas its color remained blue in the presence of Mg^{2+}. Calcon has a pK_{a2} value of 13.5 [27]; i.e., more than 50% of Calcon exists as a blue-colored species at pH 13. Therefore, it was quite reasonable that Calcon showed a clear color change from blue to purple in the presence of Ca^{2+}, as noted in Fig. 1. These results suggest that Calcon is the most suitable indicator for the measurement of Ca^{2+} at pH 13 from among these three indicators.

Consequently, 0.1 M CAPS buffer was used to attain a pH of 10 and 0.1 M KOH was selected to adjust the pH to 13. For indicators, EBT and Calcon were employed at

pH 10 and 13, respectively. Using these reagents, we prepared two μPADs, one for determining the total concentration of Ca^{2+} and Mg^{2+} (hardness) at pH 10, and the other for determining the concentration of Ca^{2+} at pH 13.

3.2. Optimization of the design

In the preliminary stages, we employed the same design as that of the μPADs for acid-base titrations. Initially, 30 μL of 0.1 M CAPS buffer was introduced into the center of the sample zone to completely fill the channels and zones of the μPAD. After drying the μPAD completely, 1 μL each of the 0.01 to 0.1 M EDTA solutions were added to the ten reaction zones in 0.01 M intervals, and 0.5 μL of 0.1% EBT was added to each of the ten detection zones. The titrations showed no clear endpoint for 0.03 M Ca^{2+} solution, e.g., the color changed from blue to purple in the zones for amounts from 0.01 to 0.03 M (Supplementary Material, Fig. S3a) while the other zones, however, only showed partial color changes, which led to incorrect results. The reading error became most apparent at the level of 0.08 M of Ca^{2+} where the detection zones up to 0.1 M should have changed color in like manner to the detection zones at the levels of 0.01 to 0.06 M (Supplementary Material, Fig. S3b).

The incorrect color change was attributed to an incomplete reaction between Ca^{2+} and EDTA due to a slow dissolution rate of the reagents including CAPS and EDTA. In the acid-base titrations using the μPAD, the acid analyte accelerated the dissolution rate of the base in the reaction zones, and vice-versa, i.e., the dissolution rate of the reagent in the reaction zone was fast enough to react with the sample solution. However, the dissolution rate of the reagents (CAPS and EDTA) was too slow to react with EDTA sufficiently in the chelate titration since the sample solution did not accelerate the

dissolution of the reagents.

To complete the complex formation in the reaction zones, we delayed the influx of the sample solution from the reaction zone into the detection zone. This was achieved by increasing the channel length between the reaction zone and the detection zone. The channel length between the reaction zone and the detection zone was 0.8 mm in the μPAD reported previously, whereas it was increased to 1.4, 2.0, and 3.0 mm. The time required to flow from the reaction zone to the detection zone was increased with increases in the length, and was 23.6 ± 2.9 s for the original design compared with 72.2 ± 2.9 s for the 3.0 mm length. Thus, the sample solution was impounded in the reaction zone for a longer period of time in the improved design with 3.0 mm than in the original version, which resulted in an increase in the time for dissolution and reaction in the reaction zones.

The holder of the μPAD was also modified to reduce the flow rate of a sample solution. In the acid-base titrations, we employed a holder that covered the surface of the μPAD and accelerated the flow rate of the sample solution due to the formation of an open channel between the μPAD and the acrylic cover plate similar to the same principle as the method to accelerate the flow rate in μPADs using razor-crafted open channels [29]. Conversely, in the chelate titration, we needed to reduce the flow rate to obtain a sufficient amount of time to dissolve the reagents in the reaction zone. Therefore, the design of the holder was changed so as not to cover the flow channels of the μPAD (Supplementary Material, Fig. S1).

3.3. Determination of Ca^{2+} and Mg^{2+}

Using the improved design, the μPAD for the chelate titrations of Mg^{2+} and Ca^{2+}

was prepared by completely filling the channels and zones with 30 μL of 0.1 M CAPS at pH 10, and then by adding 1 μL of an EDTA solution in increments of 0.01 to 0.1 M to the reaction zones and 0.5 μL of 0.1% EBT to the detection zones. Two mixtures, 10 mM Mg^{2+} + 10 mM Ca^{2+} and 30 mM Mg^{2+} + 30 mM Ca^{2+}, were titrated using the μPADs, as shown in Figs. 2a and 2b. The endpoints were observed in the detection zones by the blue color adjacent to the reaction zones containing the lowest concentration of EDTA, which corresponded to 20 mM, as shown in Fig. 2a and 60 mM in Fig. 2b. These results indicated that the μPADs permitted successful titrations for the determination of the total concentrations for Mg^{2+} and Ca^{2+}. In this study, the limits of quantification (LOQ) was defined as the lowest concentration determined by the μPADs whereas the limits of detection (LOD) was defined as the lowest concentration that changes the color of the detection zone adjacent to the reaction zone without EDTA. The LOD and LOQ were 0.5 mM for a total concentration of Mg^{2+} and Ca^{2+} (Supplementary material, Fig. S4).The μPADs for the titration of Ca^{2+} at pH 13 were prepared by completely filling the channels and zones with 0.1 M KOH instead of 0.1 M CAPS buffer, and then by adding 1 μL of an EDTA solution in increments of 0.01 to 0.1 M to the reaction zones and 0.5 μL of 0.1% Calcon to the detection zones. The same sample solutions in Figs. 2a (10 mM Mg^{2+} + 10 mM Ca^{2+}) and 2b (30 mM Mg^{2+} + 30 mM Ca^{2+}) were titrated using the μPAD, and the results are shown in Figs. 2c and 2d, which show that the sample solutions contained 10 mM Ca^{2+} and 30 mM Ca^{2+}, respectively, and both were determined using two different μPADs — one for total Mg^{2+} and Ca^{2+} and the other only for Ca^{2+}.

The μPADs for measuring 1 to 10 mM of Ca^{2+} with an interval of 1 mM were also prepared using KOH to adjust the pH to 13, and by adding 0 to 9 mM of EDTA

solutions to the reaction zones with Calcon as the indicator. When samples containing 1 to 5 mM Ca^{2+} were measured using the μPADs, the solutions containing 1 to 3 mM Ca^{2+} showed a color change only in the detection zone adjacent to the reaction zone containing no EDTA. Conversely, 4 mM and 5 mM Ca^{2+} solutions did exhibit the correct color change in the detection zones, i.e., the interval of 1 mM of Ca^{2+} was measurable in a range of more than 4 mM, even though 1 to 3 mM of Ca^{2+} could not be determined (Supplementary material, Fig. S5). The LOQ (4 mM) of the μPADs for a titration at pH 13 was slightly poorer than that for a titration at pH 10 since the measurable lowest concentration of Ca^{2+} was 4 mM, which was 8-fold higher than its measureable concentration at pH 10 (0.5 mM). Therefore, the μPADs can determine the total concentration of Mg^{2+} and Ca^{2+} in an amount higher than 1 mM, whereas Ca^{2+} concentrations lower than 4 mM are immeasurable. The LOD at pH 13 was 1 mM which was also slightly larger than 0.5 mM at pH 10 due to adsorption of Ca^{2+} on the paper substrate.

It was noteworthy that concentrations of more than 4 mM were distinguishable at an interval of 1 mM, and we were able to discriminate between the solutions containing 4 mM and 5 mM of Ca^{2+} at pH 13. This fact made it seem quite strange that the interval of 1 mM of Ca^{2+} was measurable in the range of more than 4 mM, although 1 to 3 mM of Ca^{2+} could not be determined. To clarify this phenomenon, we added 0.5 μL of Calcon to the sample, reaction and detection zones at pH 13, and then solutions of 1~5 mM of Ca^{2+} were introduced into the sample zone while EDTA was absent from the reaction zones. In the sample zone only, 1 mM Ca^{2+} showed a color change, i.e., 30 μL of 1 mM Ca^{2+} (30 nmol of Ca^{2+}) was completely retained in the sample zone (Supplementary Material, Fig. S6). The color changes spread to the reaction and

detection zones as the concentration of Ca^{2+} was increased(Supplementary Material, Fig. S6). These results indicated that Ca^{2+} could not reach the detection zones at concentrations lower than 3 mM at pH 13 even when the reaction zones contained no EDTA. Therefore, free Ca^{2+} was adsorbed onto the paper substrate at a pH of 13, which was probably due to the dissociated hydroxyl groups of cellulose (the p*K*a value of glucose is known to be 12.28) [30], although the dissociation constant is unknown. The adsorption of Ca^{2+} in the sample zone and in the reaction zones would have been saturated by the 3 mM of free Ca^{2+} since concentrations higher than 4 mM were measurable at pH 13.

The μPADs employed in Fig. 2 were prepared for determining a concentration range of 10 to 100 mM. The μPADs need to be prepared so as to allow the sample concentration to fall into the range of the EDTA concentrations added to the reaction zones. When we measure a few mM of a sample, 1 to 10 mM EDTA solutions must be added to the reaction zones, resulting in data with 1 significant figure. Conversely, if the concentration of the sample contains 10 to 20 mM of the metal ion, we can prepare the μPAD using the EDTA solutions with 10 to 20 mM at an interval of 1 mM. In this case, we can determine the concentration of the sample to 2 significant figures. Therefore the concentrations obtained by the μPADs are digital values restricted by the concentration interval of EDTA added to the reaction zones. This feature of the μPAD requires no skill in order to find the endpoint and avoid misreading in the titrations since the concentration can be judged only by the position of the detection zone indicating the endpoint.

The developed μPADs have several advantages superior to commercially available paper strips for measuring the total hardness of water. With paper strips, the hardness of

a sample is measured by a color intensity generated by the formation of a colored complex. To determine the hardness, we have to compare the result with a reference which represents the relationship between the color intensity and the concentration range, e.g., a paper strip reports that the hardness of the sample is <55, >90, >180, >270, >360, or >445 ppm. This method could cause mistakes originating from the subjective view of an observer. In addition, a paper strip cannot determine the concentrations of Ca^{2+} and Mg^{2+} independently. Conversely, the μPADs permit the determination of the exact concentrations for both Ca^{2+} and Mg^{2+} and lead to no reading errors since the judgement of the color change is clearer than the comparison of the color intensity in the paper strip.

3.4. Interference

In the classic titrations, heavy metal ions influence the titration results since several metal ions form chelates with EDTA and the indicator. Therefore, the interference of a heavy metal was investigated using Fe^{3+} as a possible interference in the determination of natural water samples. Sample solutions with 1, 10, and 100 ppm Fe^{3+} were applied to the μPADs with 0 to 90 mM of EDTA in the reaction zones at 10 mM interval using EBT as the indicator (pH 10). The solutions of 1 ppm Fe^{3+} changed the color of EBT in the detection zone when the reaction zones contained no EDTA, despite a much lower concentration (corresponding to 18 μM) of Fe^{3+} than the LOD of Ca^{2+} and Mg^{2+} (0.5 mM). Obviously, Fe^{3+} is a serious interfering substance for the μPAD.

In the classic titration, KCN is frequently employed for masking many heavy metal ions [27]. Thus, we added 30 μL of 10% KCN in all channels and zones after drying 0.1 M CAPS. Sample solutions of 40 mM Ca^{2+} with 100 to 500 ppm Fe^{3+} were titrated

using the μPADs treated with KCN. In the presence of KCN, no interference was observed up to 500 ppm (8.95 mM) of Fe^{3+}. To apply the μPADs to the determination of practical samples, especially to natural water samples, the addition of KCN will be effective to exclude the interference of heavy metal ions since the concentration levels in natural water are known to be as low as 0.5−50 μM [31].

3.5. Practical analysis

In order to demonstrate practical applicability of the μPADs, commercially available mineral water, river water, and seawater were titrated using both a classic chelate titration and the μPADs. The results are summarized in Table 1. The total concentrations of Mg^{2+} and Ca^{2+} in the mineral water samples were successfully determined at 3.2 and 19 mM using classic titration and 3 and 20 mM via the μPADs, which was in good agreement. Using the μPADs, the concentration of Ca^{2+} in mineral water 1 was below the detectable concentration limit at pH 13, and the concentration of Mg^{2+} in mineral water 2 were also undetectable due to its low concentration (both the hardness and the concentration of Ca^{2+} were found to be 20 mM).

The river water samples were taken at three different sites near the estuary of the Asahigawa River: at a point 0.2 km away from the estuary (Site 1), at the estuary (Site 2), and at the bay (Site 3). The titration results using the μPADs are shown in Fig. S7 of the Supplementary Material. For these samples, the total concentrations obtained by the μPADs (5 mM) were also consistent with those determined by classic titration (Table 1), although the concentrations of Ca^{2+} were too low to be determined by the μPADs.

The results for the determination of the seawater sample collected at the Shimotsui fishery harbor are shown in Fig. 3. As shown in Fig. 3a, when using the μPAD at pH

10 without KCN, the color in all the detection zones changed to purple. To prevent interference from heavy metal ions, we added 30 μL of 10% KCN, as described in the section 3.4. Fig. 3b shows the titration at pH 10 by the μPAD containing KCN. The endpoint was clearly found at a concentration of 40 mM, which meant the total concentration of Mg^{2+} and Ca^{2+} was 40 mM. As shown in Table 1, the total concentration of Mg^{2+} and Ca^{2+} obtained by classic titration were 44 mM, which was in good agreement with the results shown in Fig. 3b. The concentration of Ca^{2+} determined via the μPAD was 10 mM (Fig. 3c), which also was consistent with the results of classic titration (11 mM). Furthermore, we prepared the μPAD for a concentration range of from 4 to 12 mM in order to precisely determine the concentration of Ca^{2+}, and the result at 11 mM (Fig. 3d) was similar to that via classic titration. The titrations were attempted 5 times, and four of these resulted in 11 mM with one resulting in 12 mM (mean value, 11.2 mM). These results suggest that the μPADs are reliable for the determination of Ca^{2+} and Mg^{2+} in practical samples since the average concentrations of Ca^{2+} and Mg^{2+} in ocean water are 10.3 and 53.2 mM, respectively [31].

It should be emphasized that the results of the μPADs represent excellent reproducibility as noted by the standard deviations in Table 1 of zero with the exception of the concentration of Ca^{2+} in the seawater sample. Even for the seawater sample, only one in five measurements showed a 1 mM difference, although the origin of the error is unclear. The μPADs certainly make the operations of the titrations for Ca^{2+} and Mg^{2+} easy and reduce the experimental errors due to simple detection of the endpoint.

4. Conclusions

We demonstrated successful titrations of Ca^{2+} and Mg^{2+} using μPADs prepared

for measurements at pH 10 and pH 13. The μPADs were superior to a commercially available paper strip for a measurement of the hardness in water samples, because we were able to determine the exact concentrations of both Ca^{2+} and Mg^{2+} using the μPADs while the commercially available paper strip permitted only a range of hardness that corresponded to the total concentration of Ca^{2+} and Mg^{2+}. In addition, the results of the μPADs were digitized, which lessened the chances for a misreading.

The results of this research underscored several unique characteristics of filter paper. (i) The amount of time required for dissolution of the buffer components and chelating reagents deposited in the zones was a key to the success of the titrations, and increasing the channel length between the reaction and detection zones efficiently dissolved the reagents and helped complete the complex formation reaction. (ii) At pH 13, the EBT showed a blue color, even though it was purple in solution, which could be attributed to the interactions between EBT and the hydroxyl groups of cellulose. (iii) The adsorption of Ca^{2+} occurred at pH 13 due to the partial dissociation of the hydroxyl groups of cellulose under the strong alkaline conditions, and, as a consequence, it was difficult to determine the concentrations of Ca^{2+} that were lower than 4 mM.

We also successfully analyzed practical samples of mineral water, river water, and seawater. The concentrations determined by the μPADs were in good agreement with those obtained by classic titrations when KCN was employed as a masking agent. Therefore, the μPADs would be more convenient than classic titration for determinations of Ca^{2+} or Mg^{2+} in terms of lightness, less expense, transportability, and ease of operation.

Acknowledgements

This research was supported by Grants-in-Aid for Scientific Research, Scientific Research (B) (No. 26288067) from the Japan Society for the Promotion of Science (JSPS).

References

[1] A. W. Martinez, S. T. Phillips, M. J. Butte, G. M. Whitesides, Patterned paper as a platform for inexpensive, low-volume, portable bioassays, Angew. Chem., Int. Ed. 46 (2007) 1318−1320.

[2] A. W. Martinez, S. T. Phillips, G. M. Whitesides, Diagnostics for the developing world: microfluidic paper-based analytical devices, Anal. Chem. 82 (2010) 3–10.

[3] H. Noh, S. T. Phillips, Fluidic timers for time-dependent, point-of-care assays on paper, Anal. Chem. 82 (2010) 8071–8078.

[4] A. K. Yetisen, M. S. Akran, C. R. Lowe, Paper-based microfluidic point-of-care diagnostic devices, Lab Chip 13 (2013) 2210–2251.

[5] D. M. Cate, J. A. Adkins, J. Mettakoonpitak, C. S. Henry, Recent developments in paper-based microfluidic devices, Anal. Chem. 87 (2015) 19−41.

[6] C. M. Cheng, A. W. Martinez, J. Gong, C. R. Mace, S. T. Phillips, E. Carrilho, K. A. Mirica, G. M. Whitesides, Paper-based ELISA, Angew. Chem., Int. Ed. 122 (2010) 4881−4884.

[7] M. M. Mentele, J Cunningham, K. Koehler, J. Volckens, C. S. Henry, Microfluidic paper-based analytical device for particulate metals, Anal. Chem. 84 (2012) 4474−4480.

[8] A. A. Weaver, H. Reiser, T. Barstis, M. Benvenuti, D. Ghosh, M. Hunckler, B. Joy, L. Koenig, K. Raddell, M. Lieberman, Paper analytical devices for fast field screening

of beta lactam antibiotics and antituberculosis pharmaceuticals, Anal. Chem. 85 (2013) 6453−6460.

[9] P. Rattanarat, W. Dungchai, W. Siangproh, O. Chailapakul, C. S. Henry, Sodium dodecyl sulfate-modified electrochemical paper-based analytical device for determination of dopamine levels in biological samples, Anal. Chim. Acta 744 (2012) 1−7.

[10] J. Lankelma, Z. Nie, E. Carrilho, G. M. Whitesides, Paper-based analytical device for electrochemical flow-injection analysis of glucose in urine, Anal. Chem. 84 (2012) 4147−4152.

[11] M. Santhiago, J. B. Wydallis, L. T. Kubota, C. S. Henry, Construction and electrochemical characterization of microelectrodes for improved sensitivity in paper-based analytical devices, Anal. Chem. 85 (2013) 5233−5239.

[12] K. Yamada, S. Takaki, N. Komuro K. Suzuki, D. Citterio, An antibody-free microfluidic paper-based analytical device for the determination of tear fluid lactoferrin by fluorescence sensitization of Tb^{3+}, Analyst 139 (2014) 1637–1643.

[13] L. Ge, S. Wang, X. Song, S. Ge, J. Yu, 3D origami-based multifunction-integrated immunodevice: low-cost and multiplexed sandwich chemiluminescence immunoassay on microfluidic paper-based analytical device, Lab Chip 12 (2012) 3150–3158.

[14] W. Liu, C. L. Cassano, X. Xu, Z. H. Fan, Laminated paper-based analytical devices (LPAD) with origami-enabled chemiluminescence immunoassay for cotinine detection in mouse serum, Anal.Chem. 85 (2013) 10270−10276.

[15] L. Ge, J. Yan, X. Song, M. Yan, S. Ge, J. Yu, Three-dimensional paper-based electrochemiluminescence immunodevice for multiplexed measurement of biomarkers and point-of-care testing, Biomaterials 33 (2012) 1024−1031.

[16] P. Rattanarat, W. Dungchai, D. Cate, J. Volckens, O. Chailapakul, C. S. Henry, Multilayer paper-based device for colorimetric and electrochemical quantification of metals, Anal. Chem. 86 (2014) 3555−3562.

[17] B. M. Jayawardane, S. Wei, I. D. McKelvie, S. D. Kolev Microfluidic paper-based analytical device for the determination of nitrite and nitrate, Anal. Chem. 86 (2014) 7274–7279.

[18] H. Asano, Y. Shiraishi, Development of paper-based microfluidic analytical device for iron assay using photomask printed with 3D printer for fabrication of hydrophilic and hydrophobic zones on paper by photolithography, Anal. Chim. Acta 883 (2015) 55–60.

[19] K. Ogawa and T. Kaneta, Determination of iron ion in the water of a natural hot spring using microfluidic paper-based analytical devices, Anal. Sci. 32 (2016) 32−34.

[20] N. Lopez-Ruiz, V. F. Curto, M. M. Erenas, F. Benito-Lopez, D. Diamond, A. J. Palma, L. F. Capitan-Vallvey, Smartphone-based simultaneous pH and nitrite colorimetric determination for paper microfluidic devices, Anal. Chem. 86 (2014) 9554−9562.

[21] S. Karita, T. Kaneta, Acid-base titrations using microfluidic paper-based analytical devices, Anal. Chem. 86 (2014) 12108–12114.

[22] D. M. Cate, W. Dungchai, J. C. Cunningham, J. Volckens, C. S. Henry, Simple, distance-based measurement for paper analytical devices, Lab Chip 13 (2013) 2397−2404.

[23] K. Yamada, T. G. Henares, K. Suzuki, D. Citterio, Distance-based tear lactoferrin assay on microfluidic paper device using interfacial interactions on surface-modified cellulose, ACS Appl. Mater. Interfaces 7 (2015) 24864−24875.

[24] N. M. Myers, E. N. Kernisan, M. Lieberman, Lab on paper: iodometric titration on a printed card, Anal. Chem. 87 (2015) 3764−3770.

[25] C. K. Camplisson, K. M. Schilling, W. L. Pedrotti, H. A. Stoneb, A. W. Martinez, Two-ply channels for faster wicking in paper-based microfluidic devices, Lab Chip 15 (2015) 4461–4466.

[26] E. Carrilho, A. W. Martinez and G. M. Whitesides, Understanding wax printing: a simple micropatterning process for paper-based microfluidics, Anal. Chem. 81 (2009) 7091−7095.

[27] H. A. Flaschka and A. J. Jr. Barnard, Titrations with EDTA and Related Compounds. In Comprehensive Analytical Chemistry, Volume IB Classical Analysis; C. L. Wilson and D. W. Eds. Wilson; Elsevier: Amsterdam, London, New York, Princeton, 1960; pp 322−328.

[28] J. Patton and W. Reeder, New indicator for titration of calcium with (ethylenedinitrilo) tetraacetate, Anal. Chem. 28, (1956) 1026−1028.

[29] D. L. Giokas, G. Z. Tsogas and A. G. Vlessidis, Programming fluid transport in paper-based microfluidic devices using razor-crafted open channels, Anal. Chem. 86 (2014) 6202−6207.

[30] M. R. Hardy and J. S. Rohrer, High-pH Anion-Exchange Chromatography (HPAEC) and Pulsed Amperometric Detection (PAD) for Carbohydrate Analysis. In Comprehensive Glycoscience, Volume 2; J. P. Kamerling Editor-in-Chief.; Elsevier: Amsterdam, Boston, Heidelberg, London, New York, Oxford, Paris, San Francisco, Singapore, Sydney, Tokyo, 2007; pp 303−327.

[31] F. J. Millero, Chemical Oceanography, 3rd Ed.; CRC Press: Boca Raton, London, New York, 2006; pp 89−92.

Table 1. Determination of Ca^{2+} and Mg^{2+} in practical samples

		Classic Titration*	μPAD*
Mineral water 1	Mg^{2+} + Ca^{2+}/ mM	3.2±0.0089	3±0
	Ca^{2+}/ mM	2.2±0.0089	Undetectable
Mineral water 2	Mg^{2+} + Ca^{2+}/ mM	19.1±0.0084	20±0
	Ca^{2+}/ mM	16±0.011	20±0
River water (site 1)	Mg^{2+} + Ca^{2+}/ mM	5.3±0.0071	5±0
	Ca^{2+}/ mM	1.2±0.011	Undetectable
River water (site 2)	Mg^{2+} + Ca^{2+}/ mM	5.3±0.0055	5±0
	Ca^{2+}/ mM	1.2±0	Undetectable
Sea water (site 3)	Mg^{2+} + Ca^{2+}/ mM	5.5±0.0089	5±0
	Ca^{2+}/ mM	1.4±0.0071	Undetectable
Sea water	Mg^{2+} + Ca^{2+}/ mM	44±0.0071	40±0
	Ca^{2+}/ mM	11±0.0045	11.2±0.45

*Mean value ± standard deviation of five titrations.

Figure legends

Figure 1. Color of indicators at pH 13 in solution and on a μPAD. (a) The concentrations of the indicators were 0.1(w/v)% in methanol. Initially, 30 μL of KOH was applied to the μPAD so as to completely fill the channels and zones. After drying, 0.5 μL of NN, EBT, or Calcon was added to each of the detection zones, and then 0.5 μL of either a 10 mM Ca^{2+} solution or a 10 mM Mg^{2+} solution was dropped into the detection zones.

Figure 2. Chelate titration of Ca^{2+} using the μPAD. The distance between the reaction zone and the detection zone was 3 mm. (a) 10 mM Ca^{2+} + 10 mM Mg^{2+} at pH 10, (b) 30 mM Ca^{2+} + 30 mM Mg^{2+} at pH 10, (c) 10 mM Ca^{2+} + 10 mM Mg^{2+} at pH 13, (d) 30 mM Ca^{2+} + 30 mM Mg^{2+} at pH 13. EDTA solutions with 0 to 90 mM were added to the reaction zones at the interval of 10 mM. The numbers of the zones indicate the concentrations (mM) of EDTA solutions added to the reaction zones. Buffer, (a) and (b) 0.1 M CAPS, (c) and (d) 0.1 M KOH; indicator, (a) and (b) EBT, (c) and (d) Calcon. The color of each detection zone is indicated by B (blue) or P (Purple).

Figure 3. Titrations of a seawater sample. Conditions: (a) pH 10 without KCN, indicator, EBT; (b) pH 10 with KCN, indicator, EBT; (c) and (d) pH 13 with KCN, indicator, Calcon. In (c), EDTA solutions with 0 to 90 mM were added to the reaction zones at the interval of 10 mM. In (d), EDTA solutions with 0 to 12 mM were added to the reaction zones in intervals of 1 mM. The numbers of the zones indicate the concentrations (mM) of EDTA solutions added to the reaction zones. The concentrations of EDTA added to the reaction zones are indicated by the number printed on the μPADs. The color of each

detection zone is indicated by B (blue) or P (Purple).

Figure 1

Click here to download high resolution image

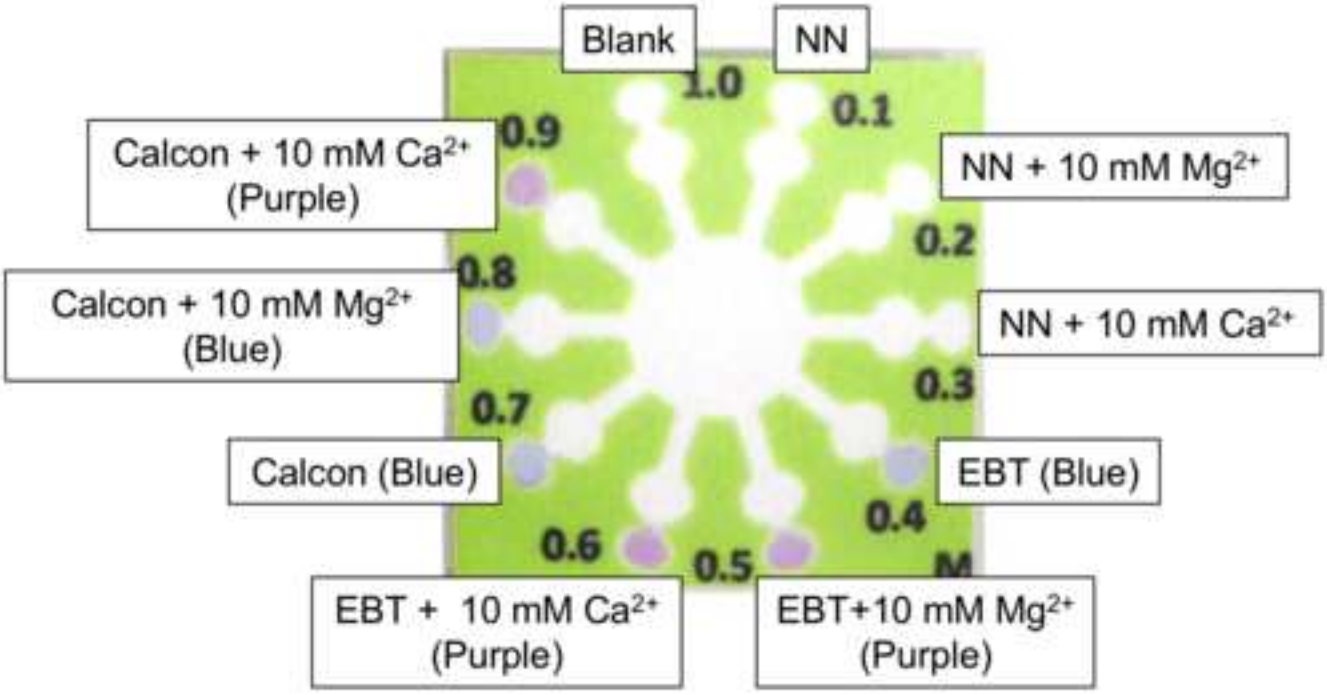

Figure 2

Click here to download high resolution image

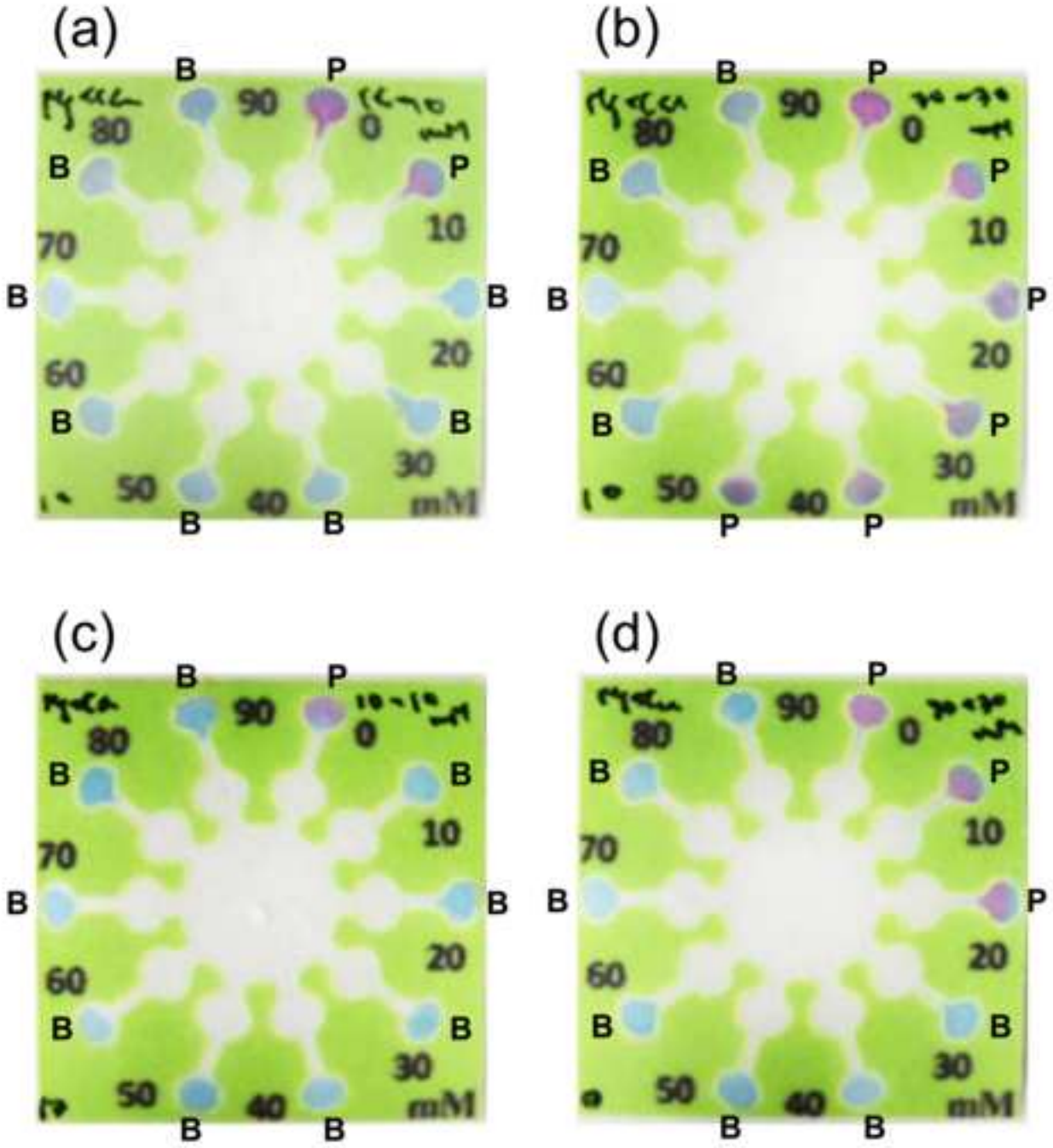

Figure 3

Click here to download high resolution image